ERDC TN-SWWRP-09-4
May 2009

Considerations for Stationary Ice Covered Flows in Adaptive Hydraulics (ADH)

by Gary L. Brown, Gaurav Savant, Charlie Berger, and David S. Smith

PURPOSE: This System-Wide Water Resources Program (SWWRP) technical note presents the theoretical development and implementation of the equations and techniques necessary to simulate stationary ice-covered flow in ADaptive Hydraulics (ADH). This implementation includes the application of a surface pressure field to simulate the weight of floating ice cover on the flow, as well as a method developed at the U.S. Army Engineer Research and Development Center (ERDC) for the calculation of drag resulting from combined bed roughness and ice cover.

BACKGROUND: The presence of ice cover over flowing water complicates the hydraulic properties of the flow by modifying the available flow cross-sectional area (via the floating ice cover), and by modifying the resistance to flow (by increasing the surface area available to shear forces and contributing unique roughness characteristics associated with the ice cover to the development of the shear profile) (Ashton 1986). The two-dimensional shallow-water (SW2) module of ADH has been extended to include changes to the flow due to the pressure imposed by an ice field as well as modifications to the shear forces. The techniques employed to account for these changes are described in detail in this technical note.

SHEAR STRESS INDUCED BY BOTH BED AND ICE COVER: In general, the presence of ice cover significantly affects the hydraulic roughness associated with a flow. If one applies classic hydraulic velocity profile theory to the ice cover problem, the complete velocity profile can be represented by two hydraulically independent profiles, which share a single, maximum velocity (for a review of classical hydraulic theory, see Schlichting 1979). These profiles divide the total flow into two distinct regions, the ice region and the bed region. The ice region and the bed region are the flow regions above and below the maximum velocity line, respectively (Figure 1).

Several researchers have questioned the validity of this two-layer theory (e.g., Ettema 2002). The classical theory dictates that the eddy viscosity coinciding with the maximum velocity should be exactly zero, but observations indicate this eddy viscosity is generally non-zero (Krishnappan 1983). Also, observations of the shear stress profile indicate that the location of zero shear stress does not necessarily coincide with the maximum velocity (Parthasarathy and Muste 1994). These observations imply that, contrary to the claims of classical theory, some energy is exchanged between profiles, and hence, the profiles are not hydraulically independent.

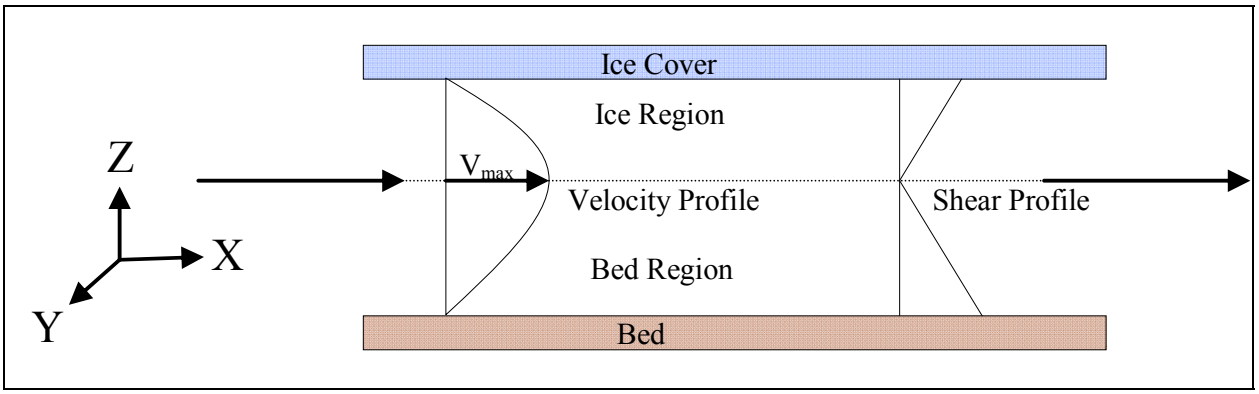

Figure 1. Schematic Representation of the Velocity and Shear Profiles under Ice Cover

In order to develop a new expression for shear stress under ice cover, the classical hydraulic theory is assumed valid and the classical theory for turbulent rough flow between two parallel surfaces with different hydraulic roughnesses is developed. An approximation term is added for the cross-profile exchange of turbulent shear by assuming that this quantity is small relative to the total drag and can be approximated with a linear superposition of a correction term derived from the classical theory.

Approach. First, the classical theory for turbulent rough flow between two parallel surfaces with different hydraulic roughnesses is developed. The following three assumptions arise from the classical theory:

1. The ice region and bed region have the same maximum velocity, which is located at the junction of the profiles.
2. Since the vertical velocity gradient at the maximum velocity height is zero, the shear stress at the maximum velocity height must also be zero.
3. Since no energy can be exchanged across a horizontal plane of zero shear stress, the two velocity profiles are hydraulically independent. Therefore, the total shear is equal to the sum of ice and bed shear stresses, which can be evaluated independently.

$$\tau_x = \tau_{BED.x} + \tau_{ICE.x} \tag{1}$$

$$\tau_y = \tau_{BED.y} + \tau_{ICE.y} \tag{2}$$

The shear stresses in x- and y-directions are given as follows:

$$\tau_{BED.x} = \frac{1}{2}\rho C_{D.BED}\left(\alpha_{BED} v_x\right)\sqrt{\left(\alpha_{BED} v_x\right)^2 + \left(\alpha_{BED} v_y\right)^2} + \tau_{CPE.x} \tag{3}$$

$$\tau_{BED.y} = \frac{1}{2}\rho C_{D.BED}\left(\alpha_{BED} v_y\right)\sqrt{\left(\alpha_{BED} v_x\right)^2 + \left(\alpha_{BED} v_y\right)^2} + \tau_{CPE.y} \tag{4}$$

$$\tau_{ICE.x} = \frac{1}{2}\rho C_{D.ICE}\left(\alpha_{ICE} v_x\right)\sqrt{\left(\alpha_{ICE} v_x\right)^2 + \left(\alpha_{ICE} v_y\right)^2} - \tau_{CPE.x} \tag{5}$$

$$\tau_{ICE.y} = \frac{1}{2}\rho C_{D.ICE}\left(\alpha_{ICE} v_y\right)\sqrt{\left(\alpha_{ICE} v_x\right)^2 + \left(\alpha_{ICE} v_y\right)^2} - \tau_{CPE.y} \tag{6}$$

$$v_{MAX.BED} = \frac{1}{\kappa}\ln\left(\beta_{BED}\right)u_{f.BED} \tag{7}$$

$$v_{MAX.ICE} = \frac{1}{\kappa}\ln\left(\beta_{ICE}\right)u_{f.ICE} \tag{8}$$

$$u_{f.BED} = \sqrt{\frac{\tau_{BED}}{\rho}} \tag{9}$$

$$u_{f.ICE} = \sqrt{\frac{\tau_{ICE}}{\rho}} \tag{10}$$

$$\beta_{BED} = 29.7\frac{z_{mv}}{k_{BED}} + 1 \tag{11}$$

$$\beta_{ICE} = 29.7\frac{\left(d - z_{mv}\right)}{k_{ICE}} + 1 \tag{12}$$

$$\kappa = 0.4 \tag{13}$$

Variables are defined at the end of this technical note.

Note that Equations 11 and 12 are expressions of the form of the velocity profile given by Christensen (1972). This velocity profile is identical to the traditional velocity profile, except for the addition of the "+1" term. This additional term only has a significant effect on the profile for small values of the roughness ratio (z/k). It ensures that the velocity magnitude v is greater than zero for all possible values of z/k (the traditional profile approaches $-\infty$ for $z/k \rightarrow 0$).

According to the classical theory, the shear profile is linear for both the bed and ice profiles, and the shear at z_{mv} must equal zero (since the velocity at z_{mv} is the maximum velocity and hence, the inflection point of the total velocity profile). This assumption can be used to express the ratio of the bed and ice shear stresses as a linear function of z_{mv} and d.

Consider the force balance for the total depth:

$$\tau = \rho g d S_{EGL} \tag{14}$$

Now, consider the force balance for just the bed friction:

$$\tau_{BED} = \rho g z_{mv} S_{EGL} \tag{15}$$

Equation 15 must be the equation for the bed force, because no energy transfer can occur across the zero shear stress line, which occurs at z_{mv}. Hence, the bed shear can only resist the weight of the water from zero to z_{mv}. The remainder of the energy (from z_{mv} to d) is absorbed by the ice shear. Next, note that:

$$\tau = \tau_{BED} + \tau_{ICE} \tag{16}$$

Substituting Equation 16 into Equation 14 and divide Equation14 by Equation 15 yields:

$$\frac{z_{mv}}{d - z_{mv}} = \frac{\tau_{BED}}{\tau_{ICE}} \tag{17}$$

Combining Equations 7, 8, and 17 can obtain an equation for z_{mv}.

$$z_{mv} = \frac{1}{\left(A^2 + 1\right)} d \tag{18}$$

where:

$$A = \frac{\ln\left(\beta_{BED}\right)}{\ln\left(\beta_{ICE}\right)} \tag{19}$$

Equations 18 and 19 must be solved iteratively, but the solution converges rapidly. A good initial estimate of z_{mv} to begin the iterations is $z_{mv} = d/2$.

The location of z_{mv} is now known and is used to determine the ice and bed drag coefficients. They are found by solving Equations 3–6 for the drag coefficients, invoking Equations 9 and 10 to express the shear stresses in terms of friction velocities, and then integrating the velocity profile to derive an expression for $\alpha v/uf$ in terms of β.

$$C_{D.BED} = 2\left(\frac{\kappa\left(\beta_{BED} - 1\right)}{\left[\beta_{BED}\left\{\ln\left(\beta_{BED}\right) - 1\right\} + 1\right]}\right)^2 \tag{20}$$

$$C_{D.ICE} = 2\left(\frac{\kappa(\beta_{ICE} - 1)}{[\beta_{ICE}\{\ln(\beta_{ICE}) - 1\} + 1]}\right)^2 \tag{21}$$

The mean velocity correction factors adjust for the ratio between the mean velocities of each profile individually and the mean velocity over the entire water depth. These relationships are derived from Equations 3–6, Equations 9 and 10, as well as the ratio given in Equation 17.

$$\alpha_{BED} = \left(\frac{1}{\alpha_{IBR}\left(\frac{d - z_{mv}}{d}\right) + \frac{z_{mv}}{d}}\right) \tag{22}$$

$$\alpha_{ICE} = \left(\frac{1}{\left(\frac{d - z_{mv}}{d}\right) + \left(\frac{1}{\alpha_{IBR}}\right)\frac{z_{mv}}{d}}\right) \tag{23}$$

$$\alpha_{IBR} = \left(\frac{C_{D.BED}}{C_{D.ICE}}\left(\frac{d - z_{mv}}{z_{mv}}\right)\right)^{1/2} \tag{24}$$

Now that the classical theory has been developed, an approximate method can be derived from the classical theory to account for the energy transfer between profiles. The theoretical development given here is derived with the implicit assumption that no energy can be exchanged between velocity profiles. However, several researchers have noted that the eddy viscosity is generally nonzero at the profile interface (Krishnappan 1983). Figure 2 is a schematic of the difference between the theoretical and observed eddy viscosity profiles.

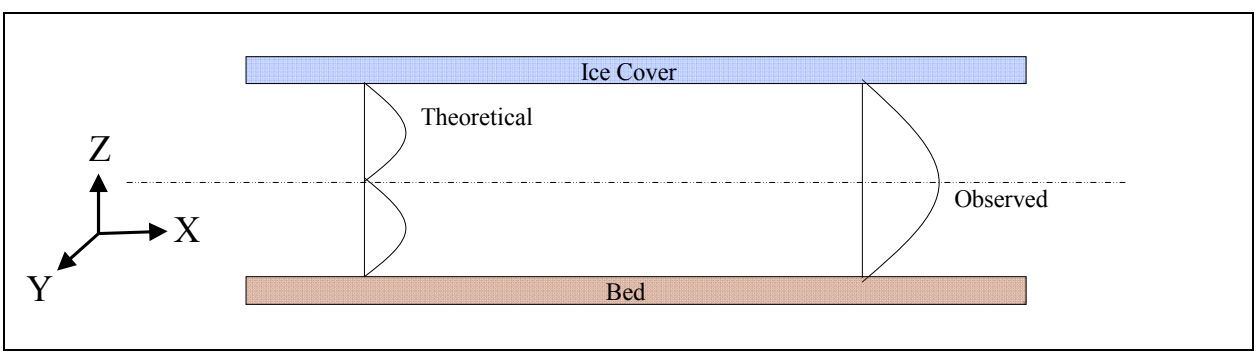

Figure 2. Schematic Representation of the Eddy Viscosity Profile under Ice Cover.

The nonzero eddy viscosity at the profile interface can cause some energy exchange across the interface. Further, the differences in the bulk momentum of each profile will cause some momentum transfer via the finite mixing length associated with the nonzero eddy viscosity at the

profile interface. This contribution is exactly zero when both profiles are identical, and increases as the difference in the profiles increases. If one makes the simplifying assumption that this bulk momentum transfer across profiles can be superimposed onto the existing theory (which was developed assuming no energy transference), the cross-profile energy exchange can be accounted for in an approximate sense with the following relations.

$$\tau_{CPE.x} \cong \rho\left(\frac{\varepsilon_{MAX.BED} + \varepsilon_{MAX.ICE}}{2}\right)\left(\frac{(\alpha_{BED} - \alpha_{ICE})}{d(1-\delta_{mv})}\right)v_x \tag{25}$$

$$\tau_{CPE.y} \cong \rho\left(\frac{\varepsilon_{MAX.BED} + \varepsilon_{MAX.ICE}}{2}\right)\left(\frac{(\alpha_{BED} - \alpha_{ICE})}{d(1-\delta_{mv})}\right)v_y \tag{26}$$

$$\varepsilon_{MAX.BED} = \frac{1}{4}\kappa u_{f.BED} z_{mv} \tag{27}$$

$$\varepsilon_{MAX.ICE} = \frac{1}{4}\kappa u_{f.ICE}(d - z_{mv}) \tag{28}$$

$$\delta_{mv} \cong 0.368 \tag{29}$$

Note that this cross-profile exchange of momentum has no effect on the total combined bed and ice shear stress, since it only passes momentum from one profile to the other. Therefore, the total shear is fully-described by the classical development, and only the partitioning of the shear between the bed and the ice cover is affected.

Comparison to Observed Data. Flume experiments for simulated ice cover were conducted by Parthasarathy and Muste (1994). Calculations using the proposed ERDC-Coastal and Hydraulics Laboratory (CHL) method were compared to these experimental results for several values of the ice-to-bed roughness ratio. The results are given in Figure 3.

The comparisons show that the proposed method is in good agreement with the experimental values for the total shear. The comparison for the partition of the shear stress between the bed and ice shear is not as good, which may indicate that the approximation of the cross-profile exchange could be improved. However, the experimenters noted that, for the case with the highest ice-to-bed-roughness ratio, they observed significant secondary currents. They postulated that these currents may have arisen from sidewall effects in the flume experiments. Such currents would increase the cross-profile exchange of momentum. Hence, the difference between the predicted and observed values may be partially attributable to the additional mixing introduced by the secondary currents. Further experimentation and analyses are needed to quantify the accuracy of the cross-profile exchange approximation.

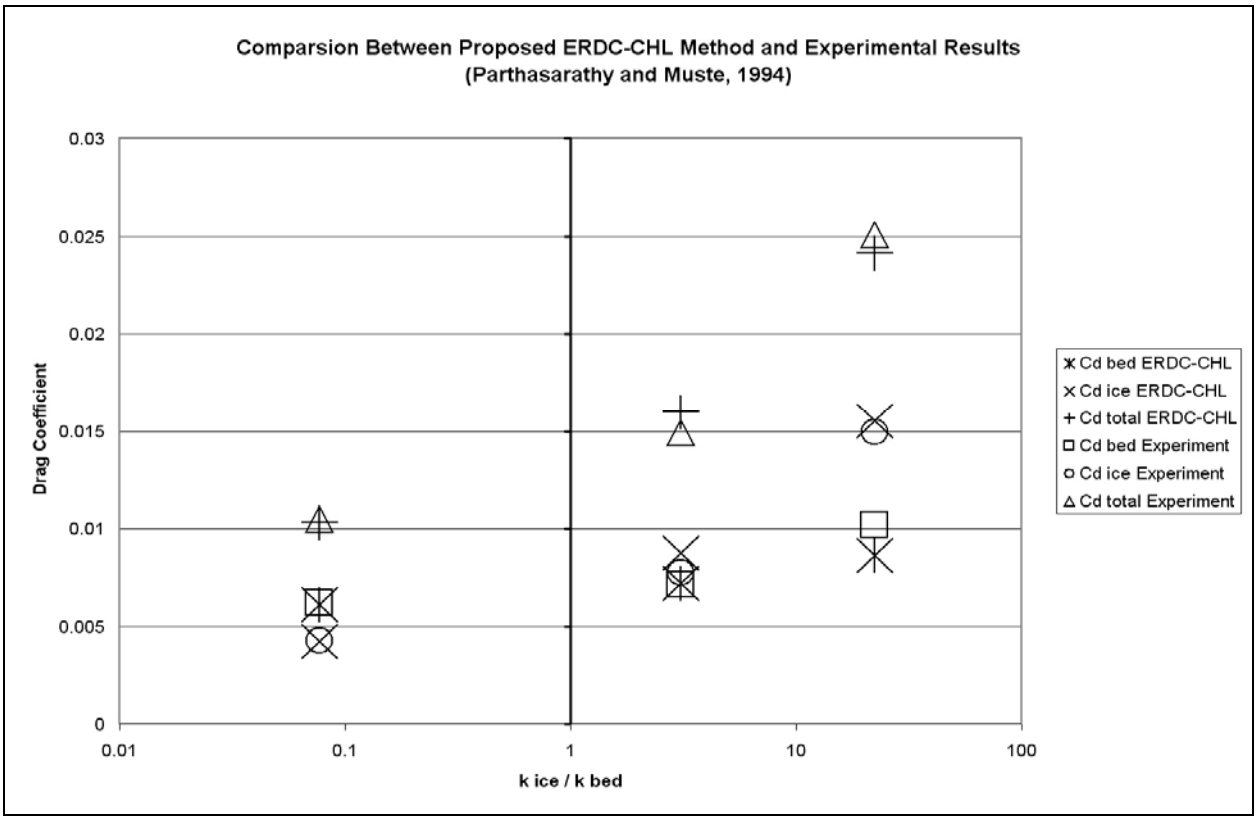

Figure 3. Comparison of the Proposed ERDC-CHL Method to the Experimental Data of Parthasarathy and Muste (1994)

Expression for Manning's n. Traditionally, the shear stress has often been expressed in terms of Manning's n. For example, the Sabaneev equation (Nezhikovskiy 1964) gives an expression for Manning's n for the composite ice-bed roughness as a function of Manning's n for the bed roughness alone. The equation is derived by invoking both velocity profile relationships and Manning's equation. It is effectively a simplified form of the more robust development given by Larsen (1969). The Sabaneev equation is given as follows:

$$\frac{n_{COMPOSITE}}{n_{BED}} = \left(\frac{n_{BED}^{3/2} + n_{ICE}^{3/2}}{2n_{BED}^{3/2}} \right)^{2/3} \tag{30}$$

An analogous relationship for the method developed in this technical note is given as follows:

$$\frac{n_{COMPOSITE}}{n_{BED}} = \left(\frac{C_{D.BED}\alpha_{BED}^2 + C_{D.ICE}\alpha_{ICE}^2}{2C_{D.BED.ONLY}} \right)^{1/2} \tag{31}$$

where:

$C_{D.BED.ONLY}$ is $C_{D.BED}$ calculated for $z_{mv} = d/2$.

IMPOSITION OF PRESSURE FIELD TO SIMULATE FLOATING ICE COVER: The presence of ice cover imposes pressure in addition to the fluid hydrostatic pressure on the fluid underneath. This pressure is a function of the ice thickness, as well as the ice density (Equation 32).

$$P_{ice} = \rho_{ice} g t_{ice} \tag{32}$$

IMPLEMENTATION INTO ADH: Implementing stationary ice effects on fluid hydraulics in ADH was done by specifying a card in the ADH boundary conditions file (*.bc) using one of two approaches – by material type or by a radius.

To specify the presence of ice by material type, one must use three cards, FR ICE, FR IRH, and FR BRH (Tables 1, 2, and 3, respectively).

Table 1
FR ICE Card Description

Field	Type	Value	Description
1	Character	FR	Card type
2	Character	Ice	Card type
3	Integer	> 0	Ice material string
4	Real	#	Ice thickness
5	Real	#	Ice density
6	Integer	0	Stationary ice

Table 2
FR IRH Card Description

Field	Type	Value	Description
1	Character	FR	Card type
2	Character	IRH	Card type
3	Real	#	Ice roughness height

Table 3
FR BRH Card Description

Field	Type	Value	Description
1	Character	FR	Card type
2	Character	BRH	Card type
3	Real	#	Bed roughness height

To specify the presence of ice by overlapping circular regions, the INS (ice node string) card must be included (Table 4), in addition to the three cards used when specifying ice by material type.

Table 4
INS Card Description

Field	Type	Value	Description
1	Character	INS	Card type
2	Real	#	X coordinate of circle center
3	Real	#	Y coordinate of circle center
4	Real	#	Radius of ice circle
5	Integer	0	Stationary ice

ADDITIONAL INFORMATION: For additional information, contact Gary L. Brown, Coastal and Hydraulics Laboratory, U.S. Army Engineer Research and Development Center, 3909 Halls Ferry Road, Vicksburg, MS 39180 at 601-634-3628, e-mail: Gary.L.Brown@usace.army.mil, or Dr. Gaurav Savant, P.E., Coastal and Hydraulics Laboratory, U.S. Army Engineer Research and Development Center, 3909 Halls Ferry Road, Vicksburg, MS 39180 at 601-634-3628, e-mail: Gaurav.Savant@usace.army.mil. This effort was funded through the System–Wide Water Resources Program (SWWRP). For information on SWWRP, please consult *https://swwrp.usace.army.mil/* or contact the Program Manager, Dr. Steven L. Ashby: Steven.L.Ashby@usace.army.mil. This SWWRP technical note should be cited as follows:

> Brown, G. L., G. Savant, C.; Berger, and D. S. Smith. 2009. *Considerations for stationary ice covered flows in ADaptive Hydraulics (ADH)* ERDC TN-SWWRP-09-4. Vicksburg, MS: U.S. Army Engineer Research and Development Center. *https://swwrp.usace.army.mil/*.

REFERENCES

Ashton, G. 1986. *River ice engineering*. Littleton, CO: Water Resources Publications.

Christensen, B. A. 1972. Incipient motion on cohesionless channel banks. *Sedimentation*. H.W. Shen, editor, Fort Collins, CO.

Ettema, R. 2002. Review of alluvial channel responses to river ice. *Journal of Cold Regions Engineering* 16(4):191-217.

Krishnappan, G. B. 1983. Suspended sediment profile for ice-covered flows. *ASCE Journal of Hydraulic Engineering* 109(3):385-399.

Larsen, P. A. 1969. Head losses caused by an ice cover on open channels. *J. Boston Society of Civil Engineer* 56(1):45-67.

Parthasarathy, R. N., and M. Muste. 1994. Velocity measurements in asymmetric turbulent channel flows. *J. Hydr. Engrg*., ASCE, 120(9):1000-1020.

Nezhikovskiy, R. A. 1964. Coefficients of roughness of bottom surface of slush ice cover. *Transactions, State Hydrologic Institute* 110:54–82.

Schlichting, H. 1979. *Boundary layer theory.* 7th ed. New York: McGraw-Hill.

VARIABLES

$C_{D.BED}$ = the bed shear stress drag coefficient
$C_{D.BED.ONLY}$ = the bed shear stress drag coefficient, assuming $z_{mv} = d/2$
$C_{D.ICE}$ = the ice shear stress drag coefficient
d = the water depth
g = the gravitational acceleration
k_{BED} = the equivalent bed roughness height
k_{ICE} = the equivalent ice roughness height
n_{BED} = the Manning's n for the bed
$n_{COMPOSITE}$ = the Manning's n for the combined ice-bed roughness
n_{ICE} = the Manning's n for the ice
P_{ice} = pressure induced by the ice cover
t_{ice} = ice thickness
v = the depth-averaged velocity magnitude
v_x = the depth-averaged velocity in the x-direction
v_y = the depth-averaged velocity in the y-direction
$v_{MAX.BED}$ = the maximum velocity for the bed profile
$v_{MAX.ICE}$ = the maximum velocity for the ice profile
$u_{f.BED}$ = the friction velocity for the bed profile
$u_{f.ICE}$ = the friction velocity for the ice profile
z_{mv} = the depth at which the maximum velocity is located (i.e. the location of the transition from the bed induced velocity profile to the ice induced velocity profile)
α_{BED} = the mean velocity correction factor for the bed shear stress
α_{ICE} = the mean velocity correction factor for the ice shear stress
α_{IBR} = the ratio of the mean velocity for the ice-induced velocity profile to the mean velocity for the bed-induced velocity profile
$\varepsilon_{MAX.BED}$ = the maximum eddy viscosity for the bed profile
$\varepsilon_{MAX.ICE}$ = the maximum eddy viscosity for the ice profile
δ_{mv} = the normalized fraction of the distance to the centroid of the velocity profile
κ = the Von Kárman constant
ρ = the density of water
ρ_{ice} = the density of ice
S_{EGL} = the slope of the energy grade line
τ_{BED} = the boundary shear at the flow-bed interface
τ_{ICE} = the boundary shear at the flow-ice interface
τ_{CPE} = the approximate cross-profile exchange of shear stress
τ = the total shear stress

NOTE: The contents of this technical note are not to be used for advertising, publication, or promotional purposes. Citation of trade names does not constitute an official endorsement or approval of the use of such products.